

Many-Body Flatband Localization

Carlo Danieli,¹ Alexei Andreanov,^{2,3} and Sergej Flach^{2,3,4}

¹Max Planck Institute for the Physics of Complex Systems, Dresden D-01187, Germany

²Center for Theoretical Physics of Complex Systems, Institute for Basic Science(IBS), Daejeon 34126, Korea

³Basic Science Program(IBS School), Korea University of Science and Technology(UST), Daejeon 34113, Korea

⁴New Zealand Institute for Advanced Study, Massey University, Auckland, Private Bag 102904, 0632 Auckland, New Zealand

(Dated: May 14, 2020)

We generate translationally invariant systems exhibiting many-body localization from All-Bands-Flat single particle lattice Hamiltonians dressed with suitable short-range many-body interactions. This phenomenon – dubbed Many-Body Flatband Localization (MBFBL) – is based on symmetries of both single particle and interaction terms in the Hamiltonian, and it holds for any interaction strength. We propose a generator of MBFBL Hamiltonians which covers both interacting bosons and fermions for arbitrary lattice dimensions, and we provide explicit examples of MBFBL models in one and two lattice dimensions. We also explicitly construct an extensive set of local integrals of motion for MBFBL models. Our results can be further generalized to long-range interactions as well as to systems lacking translational invariance.

Introduction — Understanding the lack of thermalization in quantum interacting systems has been an active topic since Anderson predicted in 1958 the absence of transport in single particle lattices due to spatial disorder [1]. This localization phenomenon has been extensively studied theoretically and experimentally [2], with the impact of interaction between localized particles as one of the main open questions. Weak interactions were predicted to preserve the absence of transport of interacting particles [3, 4] about fifty years after Anderson original work, leading to the phenomenon of *Many-Body Localization* (MBL). The study of MBL systems and their properties is nowadays a very active topic of research with several open issues and active fronts - for a survey of the state of the art, see [5, 6].

MBL was initially predicted for interacting disordered systems emerging as an interplay of disorder and weak interactions. However it was later realized that the presence of disorder is not essential, launching the search for disorder-free MBL systems. Several possible scenarios emerged as a result: from non-ergodic behavior in networks of Josephson junctions [7] to 1D fermionic lattices involving different species of particles [8] or the presence of d.c. field [9], local constraints due to gauge invariance [10], presence of a large number of conserved quantities [11, 12], quasi-periodic long-range interactions [13], among others. Some proposals also explored the connection to glasses, predicting MBL in glassy systems [14–17], *e.g.* kinetically constrained models [18] and geometrically frustrated models [19]. However, the validity of some of the proposals were later doubted, as it was shown that several disorder-free MBL systems rely on vastly different energy scales and finite-size constraints [20]. In other cases instead (*e.g.* [7]), disorder-free MBL requires high temperatures or specific strong interaction regimes, likewise the original MBL requests weak interaction regimes.

In this letter, we propose a generator of disorder-free MBL systems which is free of the above-mentioned re-

quirements (specific interaction or temperature regimes, finite-size constraints, type of many-body statistics, among others) and applies for arbitrary spatial dimensions. This generator relies on geometrical frustration of the translationally invariant single particle Hamiltonians which yields no single particle dispersion - *i.e.* all Bloch bands are dispersionless (or flat) - and suitably chosen many-body interactions. The resulting models exhibit non-ergodic behavior with lack of transport of particles for any interaction strength, and this phenomenon is dubbed *Many-Body Flatband Localization* (MBFBL). The study of networks with one or several flatbands (FB) is an active topic of research on its own. They were first discussed in the context of groundstate ferromagnetism [21], but were later identified in various other systems [22, 23] and they have been experimentally realized in several setups, using *e.g.* ultra cold atoms [24] and photonic lattices [25–27]. An important property of FB systems is the presence of compact localized states (CLS) - eigenstates with strictly finite support. These were used to systematically construct FB models [28–30] along with other methods [31–35]. Their fine-tuned character makes FB systems an ideal platform to study diverse localization phenomena in the presence of onsite disorder [36–39], DC fields [40], and nonlinearities [41, 42], among many others.

We introduce MBFBL networks formed by single particle All-Bands-Flat lattice Hamiltonians dressed with suitable short-range many-body interactions, and provide explicit examples in one and two spatial dimensions. We also discuss distinct interaction terms (including long-range interactions) in order to cover different types of particle statistics. We construct an extensive set of local integrals of motion present in MBFBL networks, and explicitly derive these integrals for some of the examples presented. We extend our generator scheme by removing the assumption of translation invariance of the lattice.

Setup — We consider a translationally invariant many-body Hamiltonian $\hat{\mathcal{H}}$ on a lattice

$$\hat{\mathcal{H}} = \hat{\mathcal{H}}_{\text{sp}} + \hat{\mathcal{H}}_{\text{int}}, \quad \hat{\mathcal{H}}_{\text{sp}} = \sum_k \hat{f}_k, \quad \hat{\mathcal{H}}_{\text{int}} = \sum_{\kappa} \hat{g}_{\kappa} \quad (1)$$

with both single particle part $\hat{\mathcal{H}}_{\text{sp}}$ and interaction $\hat{\mathcal{H}}_{\text{int}}$ written as sums of local operators \hat{f}_k and \hat{g}_{κ} . The integers k and κ label unit cells of the lattice in a direct space for two different unit cell choices A and B . We assume that the sites from one unit cell of e.g. choice A belong to *different* unit cells of choice B . Regardless of the choice, each unit cell contains ν lattices sites or single particle levels. The operators are expressed through creation and annihilation operators $\hat{c}_{k,a}^{\dagger}, \hat{c}_{k,a}$ which create or annihilate a single particle on a given lattice site k, a with $1 \leq a \leq \nu$. Then the local operators read

$$\hat{f}_k = \sum_{a,b=1}^{\nu} t_{ab} \hat{c}_{k,a}^{\dagger} \hat{c}_{k,b} + \text{h.c.} \quad (2)$$

We assume the *interaction* Hamiltonian $\hat{\mathcal{H}}_{\text{int}}$ to be two-body, so that the local operators are

$$\hat{g}_{\kappa} = \sum_{\alpha,\beta,\gamma,\delta=1}^{\nu} J_{\alpha\beta\gamma\delta} \hat{c}_{\kappa,\alpha}^{\dagger} \hat{c}_{\kappa,\beta}^{\dagger} \hat{c}_{\kappa,\gamma} \hat{c}_{\kappa,\delta} + \text{h.c.} \quad (3)$$

By the above definitions both single particle and interaction Hamiltonians are *semi-detangled* (SD) as $[\hat{f}_k, \hat{f}_{k'}] = [\hat{g}_{\kappa}, \hat{g}_{\kappa'}] = 0$ for any k, k', κ, κ' . The spectrum of the single particle eigenvalue problem with $\hat{\mathcal{H}}_{\text{sp}}$ yields ν flatbands with each being an eigenenergy of any of the local operators f_k . It follows that $\hat{\mathcal{H}}_{\text{sp}}$ enforces full localization and absence of transport. The same is true for $\hat{\mathcal{H}}_{\text{int}}$. However, because of the different unit cell choices A, B , in general it follows that $[\hat{f}_k, \hat{g}_{\kappa}] \neq 0$ for any given k and at least a pair of different values of κ (and vice versa). Consequently, the combination of both $\hat{\mathcal{H}}_{\text{sp}}$ and $\hat{\mathcal{H}}_{\text{int}}$ into \mathcal{H} in general yields transporting many-body eigenstates [43–46].

If $t_{ab} = t_{aa} \delta_{a,b}$ (with the Kronecker symbol $\delta_{a,b}$), the $\hat{\mathcal{H}}_{\text{sp}}$ is coined *fully detangled* (FD) [31] since it depends on the particle number operators $\hat{n} = \hat{c}^{\dagger} \hat{c}$ only, and does not move any particles from any lattice site to any other one. Together with $\hat{\mathcal{H}}_{\text{int}}$ being SD, the full Hamiltonian \mathcal{H} preserves full localization of particles, which is an example of *many-body flatband localization* (MBFBL). Likewise, if we assume that $J_{\alpha\beta\gamma\delta} = J_{\alpha\beta\alpha\beta} \delta_{\alpha,\gamma} \delta_{\beta,\delta}$ it follows that $\hat{\mathcal{H}}_{\text{int}}$ is FD and does not move any particles from site to site. Together with $\hat{\mathcal{H}}_{\text{sp}}$ being SD, we again arrive at the result that the full Hamiltonian \mathcal{H} lacks transporting eigenstates and is MBFBL. The relation between the FD/SD character of the Hamiltonians and the presence of MBFBL is summarized in Table I. We refer to all the other types of Hamiltonians as *non-detangled* (ND).

$\hat{\mathcal{H}}_{\text{sp}} \backslash \hat{\mathcal{H}}_{\text{int}}$	SD	FD
SD	—	MBFBL
FD	MBFBL	MBFBL

TABLE I. Existence of MBFBL for different types of single particle Hamiltonian $\hat{\mathcal{H}}_{\text{sp}}$ and interaction Hamiltonian $\hat{\mathcal{H}}_{\text{int}}$ as discussed in the main text.

We generate MBFBL Hamiltonians by choosing any of the FD/SD MBFBL models from Table (I). We then perform a unitary transformation (rotation) on each unit cell in either of the two unit cell choices A, B . This results in general in some complicated Hamiltonian with $\hat{\mathcal{H}}_{\text{sp}}$ being ND and $\hat{\mathcal{H}}_{\text{int}}$ being FD/SD, or vice versa - $\hat{\mathcal{H}}_{\text{sp}}$ being FD/SD and $\hat{\mathcal{H}}_{\text{int}}$ being ND - depending on which unit cell type the transformation was applied to. Furthermore these transformations can be chosen unit cell dependent resulting in non-translationally invariant Hamiltonians.

Conventional disordered MBL systems are known to possess an extensive set of local integrals of motion [5, 47, 48], though explicit derivations are complicated. These integrals are used to explain relevant properties of these systems. Local integrals of motion can be explicitly derived for MBFBL networks. With our proposed scheme and considering a SD single particle Hamiltonian $\hat{\mathcal{H}}_{\text{sp}}$ in \mathcal{H} (1), it follows that the expectation values of the operators $\hat{I}_k = \sum_{a=1}^{\nu} \hat{n}_{k,a}$ measure the number of particles in each local unit \hat{f}_k of $\hat{\mathcal{H}}_{\text{sp}}$. These numbers are conserved in the presence of a FD interaction $\hat{\mathcal{H}}_{\text{int}}$ (since $\hat{\mathcal{H}}_{\text{int}}$ does not move particles from one to another site). It follows that each \hat{I}_k commutes with the full Hamiltonian.

The unitary transformations used to recast $\hat{\mathcal{H}}_{\text{sp}}$ as ND yield N local integrals of motion \hat{I}_k expressed in the new basis for the generated MBFBL lattice. The very same follows if a pair of FD single particle $\hat{\mathcal{H}}_{\text{sp}}$ and a SD interaction $\hat{\mathcal{H}}_{\text{int}}$ is picked from Table I. In this case, the operators $\hat{I}_{\kappa} = \sum_{\alpha=1}^{\nu} \hat{n}_{\kappa,\alpha}$ defined in each local unit \hat{g}_{κ} of $\hat{\mathcal{H}}_{\text{int}}$ as well lead to N local integrals of motion of the MBFBL lattice after the unitary transformations have been applied. In the case of FD-FD Hamiltonians $\hat{\mathcal{H}}_{\text{sp}}, \hat{\mathcal{H}}_{\text{int}}$, the extensive set of local integrals of motion contains $\nu \times N$ elements, since each particle number operator $\hat{n}_{k,a}$ commutes with the full Hamiltonian \mathcal{H} .

Most of the generated MBFBL models, while being appealing from a mathematical point of view, could be hard to implement in experiments due to the complicated structure of the interaction $\hat{\mathcal{H}}_{\text{int}}$ spanning several unit cells. Experimental feasibility instead favors fully detangled $\hat{\mathcal{H}}_{\text{int}}$, which result e.g. from Coulomb interactions between density operators in real space [49]. Therefore we refine our generator scheme by choosing SD single particle $\hat{\mathcal{H}}_{\text{sp}}$ and FD interaction $\hat{\mathcal{H}}_{\text{int}}$, and recast $\hat{\mathcal{H}}_{\text{sp}}$ to a ND Hamiltonian via unitary transformations that keep

$\hat{\mathcal{H}}_{\text{int}}$ fully detangled. This algorithm works for any number of bands ν of $\hat{\mathcal{H}}_{\text{sp}}$, in any dimension, and any type of many-body statistics.

Results — We will now discuss concrete examples in one and two spatial dimensions. We consider the SD Hamiltonian $\hat{\mathcal{H}}_{\text{sp}}$ and conveniently restate it in the unit cell representation B of $\hat{\mathcal{H}}_{\text{int}}$. We then apply the subsequent unitary transformations. This change of unit cell introduces hopping terms between neighboring unit cells in each local Hamiltonian \hat{f}_κ . Without loss of generality, we assume nonzero hoppings between nearest-neighbor unit cells only, and we adopt the conventions used in Refs. [28, 29] for flatband networks generators. Then a possible $D = 1$ Hamiltonian $\hat{\mathcal{H}}_{\text{sp}}$ reads

$$\hat{\mathcal{H}}_{\text{sp}} = \sum_{\kappa} \hat{f}_\kappa = \sum_{\kappa} \left[\frac{1}{2} \hat{C}_\kappa^{\dagger T} H_0 \hat{C}_\kappa + \hat{C}_\kappa^{\dagger T} H_1 \hat{C}_{\kappa+1} + \text{h.c.} \right] \quad (4)$$

where we grouped the annihilation (creation) operators $\hat{c}_{\kappa,a}$ ($\hat{c}_{\kappa,a}^\dagger$) in ν -dimensional vectors \hat{C}_κ (\hat{C}_κ^\dagger). The matrices H_0, H_1 describe intra- and intercell hopping respectively, and are chosen so as to enforce the SD condition $[\hat{f}_\kappa, \hat{f}_{\kappa'}] = 0$ for all κ, κ' . We remark that this $\hat{\mathcal{H}}_{\text{sp}}$ is only one of the infinitely many realizations of a SD single particle Hamiltonian.

The FD two-body interaction Hamiltonian $\hat{\mathcal{H}}_{\text{int}}$ introduced above (1.3) is taken with the coefficients $J_{\alpha\beta\gamma\delta} = J_{\alpha\beta\alpha\beta} \delta_{\alpha,\gamma} \delta_{\beta,\delta}$ for each local component \hat{g}_κ : $J_{\alpha\beta\alpha\beta} = 1$ for $\alpha = \beta$ and $J_{\alpha\beta\alpha\beta} = 2$ for $\alpha \neq \beta$. Then $\hat{\mathcal{H}}_{\text{int}}$ is preserved as FD with the same coefficients $J_{\alpha\beta\gamma\delta}$ by any 2×2 unitary transformation

$$U_{ab} : \begin{cases} \hat{c}_{\kappa,a} = z \hat{d}_{\kappa,a} + w \hat{d}_{\kappa,b} \\ \hat{c}_{\kappa,b} = -w^* \hat{d}_{\kappa,a} + z^* \hat{d}_{\kappa,b} \end{cases} \quad (5)$$

parameterized by two complex numbers z, w such that $|z|^2 + |w|^2 = 1$ and any pair of sites $\hat{c}_{\kappa,a}, \hat{c}_{\kappa,b}$.

The resulting Hamiltonian $\hat{\mathcal{H}}_{\text{int}}$ for $\nu = 2$ bands describes a two-body interaction among the sites $\hat{a}_\kappa = \hat{c}_{\kappa,a}, \hat{b}_\kappa = \hat{c}_{\kappa,b}$

$$\begin{aligned} \hat{\mathcal{H}}_{\text{int}} &= \sum_{\kappa} [\hat{a}_\kappa^\dagger \hat{a}_\kappa^\dagger \hat{a}_\kappa \hat{a}_\kappa + \hat{b}_\kappa^\dagger \hat{b}_\kappa^\dagger \hat{b}_\kappa \hat{b}_\kappa + 2 \hat{a}_\kappa^\dagger \hat{a}_\kappa \hat{b}_\kappa^\dagger \hat{b}_\kappa] \\ &= \sum_{\kappa} [\hat{n}_{a,\kappa} + \hat{n}_{b,\kappa} - 1] [\hat{n}_{a,\kappa} + \hat{n}_{b,\kappa}] \end{aligned} \quad (6)$$

with $\hat{n}_{a,\kappa} = \hat{a}_\kappa^\dagger \hat{a}_\kappa$ and $\hat{n}_{b,\kappa} = \hat{b}_\kappa^\dagger \hat{b}_\kappa$. We refer to such interaction as an *extended Hubbard* interaction, which applies to both bosons and fermions with spin.

1D networks — We now present two concrete examples of MBFBL networks. We first start with the simplest MBFBL network with $\nu = 2$ bands. It is based on the Hamiltonian $\hat{\mathcal{H}}_{\text{sp}}$ in Eq. (4) with

$$H_0 = \begin{pmatrix} 1 & 0 \\ 0 & 0 \end{pmatrix}, \quad H_1 = \begin{pmatrix} 0 & t \\ 0 & 0 \end{pmatrix}, \quad (7)$$

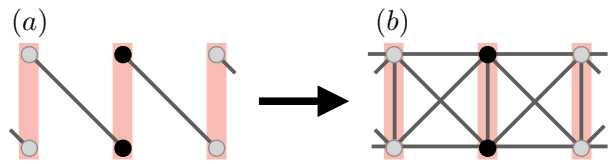


FIG. 1. (Color online) One dimensional two band MBFBL network with $\hat{\mathcal{H}}_{\text{sp}}$ SD (a) and with the cross-stitch lattice profile (b). The black circles indicate the unit cell choice, the solid lines correspond to sites connected by $\hat{\mathcal{H}}_{\text{sp}}$ before (a) and after (b) the rotation, and the red shaded rods indicate the sites connected by the extended Hubbard terms (6) of $\hat{\mathcal{H}}_{\text{int}}$.

and a free complex parameter t . It is straightforward to check that this Hamiltonian is SD and has all bands flat. Next we pick the extended Hubbard interaction $\hat{\mathcal{H}}_{\text{int}}$ (6). The structure of $\hat{\mathcal{H}}_{\text{sp}}$ and $\hat{\mathcal{H}}_{\text{int}}$ is shown in Fig. 1(a) with solid lines and red shaded rods respectively. The rotation U_{ab} (5) recasts H_0, H_1 (7) as

$$H_0 = \begin{pmatrix} |z|^2 & -zw \\ -z^*w^* & |w|^2 \end{pmatrix}, \quad H_1 = t \begin{pmatrix} zw^* & z^2 \\ -(w^*)^2 & -zw^* \end{pmatrix}, \quad (8)$$

and makes Hamiltonian $\hat{\mathcal{H}}_{\text{sp}}$ ND, while $\hat{\mathcal{H}}_{\text{int}}$ remains FD. The resulting MBFBL network is shown in Fig. 1(b). The local integrals of motion read (after the rotation)

$$\begin{aligned} \hat{I}_\kappa &= |z|^2 (\hat{n}_{a,\kappa-1} + \hat{n}_{b,\kappa}) + |w|^2 (\hat{n}_{a,\kappa} + \hat{n}_{b,\kappa-1}) \\ &\quad + z^* w (\hat{a}_{\kappa-1}^\dagger \hat{b}_{\kappa-1} - \hat{a}_\kappa^\dagger \hat{b}_\kappa) + \text{h.c.} \end{aligned} \quad (9)$$

For three bands $\nu = 3$ with operators $a_\kappa, b_\kappa, c_\kappa$ corresponding to the three sites of the unit cell, the SD Hamiltonian $\hat{\mathcal{H}}_{\text{sp}}$ (6) has the following hopping matrices

$$H_0 = \begin{pmatrix} 1 & 0 & 0 \\ 0 & 0 & t_1 \\ 0 & t_1^* & \mu \end{pmatrix}, \quad H_1 = \begin{pmatrix} 0 & 0 & t_2 \\ 0 & 0 & 0 \\ 0 & 0 & 0 \end{pmatrix}, \quad (10)$$

with two free complex (t_1, t_2) and one free real (μ) parameters. This network is shown in Fig. 2(a) with gray solid lines. The interaction $\hat{\mathcal{H}}_{\text{int}}$ consists of the extended Hubbard interaction (6) between the top and the bottom sites (a_κ, b_κ) of each plaquette (red shaded rods in Fig. 2(a)) and an additional optional onsite Hubbard interaction for the central site c_κ . Then the rotation U_{ab} (5) is applied to the pair (a_κ, b_κ) only while leaving the sites c_κ untouched. This recasts H_0, H_1 (10) into

$$H_0 = \begin{pmatrix} |z|^2 & -zw & t_1 w \\ -z^*w^* & |w|^2 & t_1 z^* \\ t_1^* w^* & t_1^* z & \mu \end{pmatrix}, \quad H_1 = t_2 \begin{pmatrix} 0 & 0 & z \\ 0 & 0 & -w^* \\ 0 & 0 & 0 \end{pmatrix} \quad (11)$$

defining a ND Hamiltonian $\hat{\mathcal{H}}_{\text{sp}}$ while the interaction $\hat{\mathcal{H}}_{\text{int}}$ remains FD. The resulting diamond-shaped MBFBL network is shown in Fig. 2(b). That diamond-shape profile

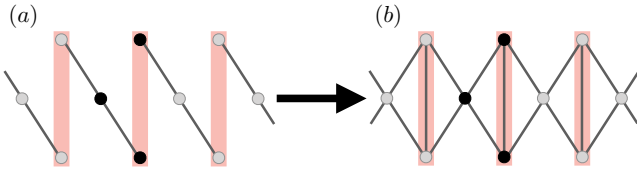


FIG. 2. (Color online) One dimensional three band MBFBL network with $\hat{\mathcal{H}}_{\text{sp}}$ SD (a) and with the diamond-shaped lattice profile (b). The black circles indicate the unit cell choice, the solid lines correspond to $\hat{\mathcal{H}}_{\text{sp}}$ before (a) and after (b) the rotations, and the red shaded rods indicate the extended Hubbard terms (6) of $\hat{\mathcal{H}}_{\text{int}}$.

has been realized in diverse experimental setups for flat-band and compact localized state studies [50–54]. Experimentally, the selective extended Hubbard interaction involving only the top and bottom sites $\hat{a}_\kappa, \hat{b}_\kappa$ of the diamond plaquette might be achieved by reducing the distance between these sites as compared to the distance to the middle site \hat{c}_κ . The parameter t_1 could be used to adjust the hoppings. The local integrals of motion \hat{I}_κ for this model are given by Eq. (9) plus the additional particle number operator $\hat{n}_{c,\kappa}$ for the central site \hat{c}_κ of the lattice, since it is unaffected by the rotation.

2D networks — Construction of higher dimensional MBFBL networks follows a procedure similar to that of 1D systems. In the simplest setting, the single particle Hamiltonian $\hat{\mathcal{H}}_{\text{sp}}$ can be taken as a straightforward extension of Eq. (4), where matrices H_1 are replaced with matrices H_0 and $H_1^{(1)}, \dots, H_1^{(D)}$ describing the intercell hopping along different spatial directions. The matrices are chosen to ensure that $\hat{\mathcal{H}}_{\text{sp}}$ is SD. Now taking a suitable FD interaction $\hat{\mathcal{H}}_{\text{int}}$, Eq. (6) or its generalizations, and picking a unitary transformation that leaves this $\hat{\mathcal{H}}_{\text{int}}$ FD, we obtain a ND Hamiltonian $\hat{\mathcal{H}}_{\text{sp}}$. The full Hamiltonian \mathcal{H} exhibits MBFBL [55].

A notable two dimensional lattice exhibiting MBFBL obtained by applying these rules is the *decorated Lieb* lattice [56]. This is a five-band $\nu = 5$ network, whose SD Hamiltonian $\hat{\mathcal{H}}_{\text{sp}}$ is shown in Fig. 3(a), with matrices $H_0, H_1^{(1)}, H_1^{(2)}$. In each unit cell, we use the extended Hubbard Hamiltonians $\hat{\mathcal{H}}_{\text{int}}$ (6) for the two site pairs indicated by red shaded rods in Fig. 3(a), and an onsite Hubbard interaction for the central site. The two rotations U_{ab} (5) applied to the highlighted pairs (leaving the central site untouched) yield a ND $\hat{\mathcal{H}}_{\text{sp}}$ shown in Fig. 3(b), and the resulting full Hamiltonian \mathcal{H} is MBFBL. The local integrals of motion for the decorated Lieb lattice can be easily derived and have similar but more involved expressions to those of the previous models (9).

Perspectives — The proposed scheme relies on the two-body Hamiltonian $\hat{\mathcal{H}}_{\text{int}}$ with onsite terms in the interaction, restricting the interacting particles to bosons or spinful fermions. However, the same construction can be implemented for spinless fermions by *e.g.* choosing local

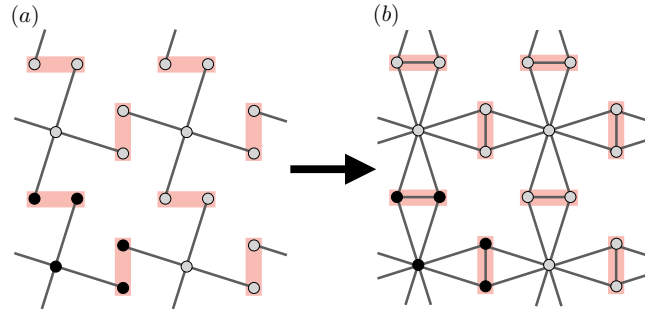


FIG. 3. (Color online) Two dimensional five band MBFBL network with $\hat{\mathcal{H}}_{\text{sp}}$ SD (a) and with the decorated Lieb lattice profile (b). The black circles indicate the unit cell choice, the solid lines correspond to $\hat{\mathcal{H}}_{\text{sp}}$ before (a) and after (b) the rotations, and the red shaded rods indicate the extended Hubbard terms (6) of $\hat{\mathcal{H}}_{\text{int}}$.

operators $\hat{g}_\kappa^\sigma = \sum_{\alpha,\beta,\gamma,\delta=1}^\nu J_{\alpha\beta\gamma\delta}^\sigma \hat{c}_{\kappa,\alpha}^\dagger \hat{c}_{\kappa+\sigma,\beta}^\dagger \hat{c}_{\kappa,\gamma} \hat{c}_{\kappa+\sigma,\delta} + h.c.$ with exclusively inter-site interaction terms between unit cell κ and unit cell $\kappa + \sigma$. In particular, $\hat{\mathcal{H}}_{\text{int}}$ is FD for $J_{\alpha\beta\gamma\delta}^\sigma = J \delta_{\alpha,\gamma} \delta_{\beta,\delta}$ and it is preserved as FD by the same transformation (5). This yields a generator of D -dimensional ν -band MBFBL lattices for spinless fermions, with the recent work of Kuno *et al.* [57] being a particular $D = 1$ $\nu = 2$ band example. The construction can be further extended to long-range all-to-all interaction Hamiltonians $\hat{\mathcal{H}}_{\text{int}}$ by setting $\hat{g}_\kappa = \sum_\sigma v_\sigma \hat{g}_\kappa^\sigma$ and even infinite-range interactions $\hat{\mathcal{H}}_{\text{int}} = J/N \sum_{\kappa \neq \kappa', a} \hat{n}_{\kappa,a} \hat{n}_{\kappa',a}$. The latter example is valid because the interaction is a function of the total density $\hat{\rho} = \sum_{\kappa,a} \hat{n}_{\kappa,a}$ only and is therefore invariant under the transformation (5).

We note that it is possible to extend the generator by abandoning the translational invariance of the Hamiltonian \mathcal{H} . We can choose the hopping parameters t_{ab} and the interaction matrix elements $J_{\alpha\beta\gamma\delta}$ in the starting Hamiltonians $\hat{\mathcal{H}}_{\text{sp}}$ and $\hat{\mathcal{H}}_{\text{int}}$ respectively to be unit cell dependent. To stick with the proposed scheme where $\hat{\mathcal{H}}_{\text{int}}$ is FD and is preserved by unitary transformations (5), the unit cell dependent terms are restrained to the SD $\hat{\mathcal{H}}_{\text{sp}}$ only (*e.g.* onsite or hopping disorder). The unitary transformations (5) used to recast $\hat{\mathcal{H}}_{\text{sp}}$ as ND induce correlations between the onsite energies of the pairs of sites involved. In the models presented - Figs.1(b), 2(b), 3(b) - these correlations are between the sites within the same red-shaded area. These correlations depend of the parameters z, w defining $U_{a,b}$ in Eq. (5). These parameters may also be chosen to vary upon changing κ if the unitary transformations considered differ from unit cell to unit cell. Let us additionally observe that the breaking of translation invariance does not destroy the existence of the extensive set of local integrals of motion - they are given by the same operators as in the translationally invariant case.

Conclusions — We have introduced a generator of Many-Body Localized disorder-free Hamiltonians by applying unitary transformations to suitably detangled Hamiltonians – a feature that assumes all-band-flat single particle Hamiltonians. This new phenomenon – coined Many-Body Flatband Localization – implies strict localization of any number of particles irrespective of dimensionality or interaction strength, and it does not require vastly different energy scales similar some models supposed to exhibit disorder-free MBL. Our work substantially extends previous studies of localization phenomena of interacting quantum many-body platforms with All-Band-Flat lattice single particle Hamiltonians [44, 46, 57–63]. In particular, we propose a flexible and general set of many-body localized systems which may be experimentally feasible. A novel and unique feature of these systems is the existence of unitary mappings that recast them into a detangled form. This very property can be employed to study the impact of additional perturbations of the proposed networks which lift MBFBL and modify the proposed local integrals of motion in a systematic and analytical form. Hence, these systems offer innovative and powerful tools to potentially perform systematic analytical studies of conventional properties of MBL networks which typically rely on heavy numerical studies.

Acknowledgments — This work was supported by the Institute for Basic Science (Project number IBS-R024-D1). SF acknowledges support by the New Zealand Institute for Advanced Study where part of this work was completed.

-
- [1] P. W. Anderson, “Absence of diffusion in certain random lattices,” *Phys. Rev.* **109**, 1492–1505 (1958).
- [2] B. Kramer and A. MacKinnon, “Localization: theory and experiment,” *Rep. Prog. Phys.* **56**, 1469–1564 (1993).
- [3] D.M. Basko, I.L. Aleiner, and B.L. Altshuler, “Metal-insulator transition in a weakly interacting many-electron system with localized single-particle states,” *Ann. Phys.* **321**, 1126 – 1205 (2006).
- [4] I. L. Aleiner, B. L. Altshuler, and G. V. Shlyapnikov, “A finite-temperature phase transition for disordered weakly interacting bosons in one dimension,” *Nat. Phys.* **6**, 900–904 (2010).
- [5] Dmitry A. Abanin and Zlatko Papić, “Recent progress in many-body localization,” *Ann. Phys.* **529**, 1700169 (2017).
- [6] Dmitry A. Abanin, Ehud Altman, Immanuel Bloch, and Maksym Serbyn, “Colloquium: Many-body localization, thermalization, and entanglement,” *Rev. Mod. Phys.* **91**, 021001 (2019).
- [7] Manuel Pino, Lev B. Ioffe, and Boris L. Altshuler, “Non-ergodic metallic and insulating phases of Josephson junction chains,” *PNAS* **113**, 536–541 (2016).
- [8] Mauro Schiulaz, Alessandro Silva, and Markus Müller, “Dynamics in many-body localized quantum systems without disorder,” *Phys. Rev. B* **91**, 184202 (2015).
- [9] M. Schulz, C. A. Hooley, R. Moessner, and F. Pollmann, “Stark many-body localization,” *Phys. Rev. Lett.* **122**, 040606 (2019).
- [10] P. Karpov, R. Verdel, Y. P. Huang, M. Schmitt, and M. Heyl, “Disorder-free localization in an interacting two-dimensional lattice gauge theory,” (2020), [arXiv:2003.04901 \[cond-mat.str-el\]](https://arxiv.org/abs/2003.04901).
- [11] A. Smith, J. Knolle, D. L. Kovrizhin, and R. Moessner, “Disorder-free localization,” *Phys. Rev. Lett.* **118**, 266601 (2017).
- [12] Adam Smith, Johannes Knolle, Roderich Moessner, and Dmitry L. Kovrizhin, “Dynamical localization in F_2 lattice gauge theories,” *Phys. Rev. B* **97**, 245137 (2018).
- [13] Rubem Mondaini and Zi Cai, “Many-body self-localization in a translation-invariant hamiltonian,” *Phys. Rev. B* **96**, 035153 (2017).
- [14] C. R. Laumann, A. Pal, and A. Scardicchio, “Many-body mobility edge in a mean-field quantum spin glass,” *Phys. Rev. Lett.* **113**, 200405 (2014).
- [15] C. L. Baldwin, C. R. Laumann, A. Pal, and A. Scardicchio, “The many-body localized phase of the quantum random energy model,” *Phys. Rev. B* **93**, 024202 (2016).
- [16] C. L. Baldwin, C. R. Laumann, A. Pal, and A. Scardicchio, “Clustering of nonergodic eigenstates in quantum spin glasses,” *Phys. Rev. Lett.* **118**, 127201 (2017).
- [17] G. Mossi, T. Parolini, S. Pilati, and A. Scardicchio, “On the quantum spin glass transition on the Bethe lattice,” *J Stat. Mech.* **2017**, 013102 (2017).
- [18] Merlijn van Horsen, Emanuele Levi, and Juan P. Garrahan, “Dynamics of many-body localization in a translation-invariant quantum glass model,” *Phys. Rev. B* **92**, 100305 (2015).
- [19] Yang Zhao and Alexei Andreanov, “in progress,”.
- [20] Z. Papi, E. Miles Stoudenmire, and Dmitry A. Abanin, “Many-body localization in disorder-free systems: The importance of finite-size constraints,” *Ann. Phys.* **362**, 714 – 725 (2015).
- [21] Andreas Mielke and Hal Tasaki, “Ferromagnetism in the Hubbard model,” *Comm. Math. Phys.* **158**, 341–371 (1993).
- [22] Daniel Leykam, Alexei Andreanov, and Sergej Flach, “Artificial flat band systems: from lattice models to experiments,” *Adv. Phys.: X* **3**, 1473052 (2018).
- [23] Daniel Leykam and Sergej Flach, “Perspective: Photonic flatbands,” *APL Phot.* **3**, 070901 (2018).
- [24] Shintaro Taie, Hideki Ozawa, Tomohiro Ichinose, Takuei Nishio, Shuta Nakajima, and Yoshiro Takahashi, “Coherent driving and freezing of bosonic matter wave in an optical Lieb lattice,” *Sci. Adv.* **1** (2015), [10.1126/sciadv.1500854](https://doi.org/10.1126/sciadv.1500854).
- [25] Seababrat Mukherjee, Alexander Spracklen, Debaditya Choudhury, Nathan Goldman, Patrik Öhberg, Erika Andersson, and Robert R. Thomson, “Observation of a localized flat-band state in a photonic Lieb lattice,” *Phys. Rev. Lett.* **114**, 245504 (2015).
- [26] Rodrigo A. Vicencio, Camilo Cantillano, Luis Morales-Inostroza, Bastián Real, Cristian Mejía-Cortés, Steffen Weimann, Alexander Szameit, and Mario I. Molina, “Observation of localized states in Lieb photonic lattices,” *Phys. Rev. Lett.* **114**, 245503 (2015).
- [27] Steffen Weimann, Luis Morales-Inostroza, Bastián Real, Camilo Cantillano, Alexander Szameit, and Rodrigo A.

- Vicencio, “Transport in sawtooth photonic lattices,” *Opt. Lett.* **41**, 2414–2417 (2016).
- [28] Wulayimu Maimaiti, Alexei Andreanov, Hee Chul Park, Oleg Gendelman, and Sergej Flach, “Compact localized states and flat-band generators in one dimension,” *Phys. Rev. B* **95**, 115135 (2017).
- [29] Wulayimu Maimaiti, Sergej Flach, and Alexei Andreanov, “Universal $d = 1$ flat band generator from compact localized states,” *Phys. Rev. B* **99**, 125129 (2019).
- [30] Wulayimu Maimaiti Maimaiti, Alexei Andreanov, and Sergej Flach, “in preparation,”.
- [31] Sergej Flach, Daniel Leykam, Joshua D. Bodyfelt, Peter Matthies, and Anton S. Desyatnikov, “Detangling flat bands into Fano lattices,” *EPL (Europhysics Letters)* **105**, 30001 (2014).
- [32] R. G. Dias and J. D. Gouveia, “Origami rules for the construction of localized eigenstates of the Hubbard model in decorated lattices,” *Sci. Rep.* **5**, 16852 EP – (2015).
- [33] Ajith Ramachandran, Alexei Andreanov, and Sergej Flach, “Chiral flat bands: Existence, engineering, and stability,” *Phys. Rev. B* **96**, 161104 (2017).
- [34] M. Röntgen, C. V. Morfonios, and P. Schmelcher, “Compact localized states and flat bands from local symmetry partitioning,” *Phys. Rev. B* **97**, 035161 (2018).
- [35] L A Toikka and A Andreanov, “Necessary and sufficient conditions for flat bands in m-dimensional n-band lattices with complex-valued nearest-neighbour hopping,” *J Phys. A: Math. Theor* **52**, 02LT04 (2018).
- [36] Daniel Leykam, Sergej Flach, Omri Bahat-Treidel, and Anton S. Desyatnikov, “Flat band states: Disorder and nonlinearity,” *Phys. Rev. B* **88**, 224203 (2013).
- [37] Joshua D. Bodyfelt, Daniel Leykam, Carlo Danieli, Xiaoquan Yu, and Sergej Flach, “Flatbands under correlated perturbations,” *Phys. Rev. Lett.* **113**, 236403 (2014).
- [38] Carlo Danieli, Joshua D. Bodyfelt, and Sergej Flach, “Flat-band engineering of mobility edges,” *Phys. Rev. B* **91**, 235134 (2015).
- [39] Daniel Leykam, Joshua D. Bodyfelt, Anton S. Desyatnikov, and Sergej Flach, “Localization of weakly disordered flat band states,” *Eur. Phys. J. B* **90**, 1 (2017).
- [40] A. R. Kolovsky, A. Ramachandran, and S. Flach, “Topological flat Wannier-Stark bands,” *Phys. Rev. B* **97**, 045120 (2018).
- [41] C. Danieli, A. Maluckov, and S. Flach, “Compact discrete breathers on flat-band networks,” *Low Temp. Phys.* **44**, 678–687 (2018).
- [42] Ajith Ramachandran, Carlo Danieli, and Sergej Flach, “Fano resonances in flat band networks,” in *Fano Resonances in Optics and Microwaves: Physics and Applications*, edited by Eugene Kamenetskii, Almas Sadreev, and Andrey Miroshnichenko (Springer International Publishing, Cham, 2018) pp. 311–329.
- [43] Julien Vidal, Rémy Mosseri, and Benoit Douçot, “Aharonov-Bohm cages in two-dimensional structures,” *Phys. Rev. Lett.* **81**, 5888–5891 (1998).
- [44] Julien Vidal, Benoit Douçot, Rémy Mosseri, and Patrick Butaud, “Interaction induced delocalization for two particles in a periodic potential,” *Phys. Rev. Lett.* **85**, 3906–3909 (2000).
- [45] Simon Tilleke, Mirko Daumann, and Thomas Dahm, “Nearest neighbour particle-particle interaction in fermionic quasi one-dimensional flat band lattices,” *Zeitschrift für Naturforschung A*, 20190371 (2020).
- [46] Carlo Danieli, Mithun Thudiyangal, Alexei Andreanov, and Sergej Flach, “Caging of short-range interactions in all bands flat lattices: Part I,” (2020), [arXiv:2004.11871 \[cond-mat.quant-gas\]](https://arxiv.org/abs/2004.11871); “Caging of short-range interactions in all bands flat lattices: Part II,” (2020), [arXiv:2004.11880 \[cond-mat.quant-gas\]](https://arxiv.org/abs/2004.11880).
- [47] Maksym Serbyn, Z. Papić, and Dmitry A. Abanin, “Local conservation laws and the structure of the many-body localized states,” *Phys. Rev. Lett.* **111**, 127201 (2013).
- [48] V. Ros, M. Mller, and A. Scardicchio, “Integrals of motion in the many-body localized phase,” *Nucl. Phys. B* **891**, 420 – 465 (2015).
- [49] John M Ziman, *Principles of the Theory of Solids* (Cambridge university press, 1972).
- [50] Sebabrata Mukherjee and Robert R. Thomson, “Observation of localized flat-band modes in a quasi-one-dimensional photonic rhombic lattice,” *Opt. Lett.* **40**, 5443–5446 (2015).
- [51] Sebabrata Mukherjee and Robert R. Thomson, “Observation of robust flat-band localization in driven photonic rhombic lattices,” *Opt. Lett.* **42**, 2243–2246 (2017).
- [52] Sebabrata Mukherjee, Marco Di Liberto, Patrik Öhberg, Robert R. Thomson, and Nathan Goldman, “Experimental observation of Aharonov-Bohm cages in photonic lattices,” *Phys. Rev. Lett.* **121**, 075502 (2018).
- [53] Shiqiang Xia, Carlo Danieli, Wenchao Yan, Denghui Li, Shiqi Xia, Jina Ma, Hai Lu, Daohong Song, Liqin Tang, Sergej Flach, and Zhigang Chen, “Observation of quincunx-shaped and dipole-like flatband states in photonic rhombic lattices without band-touching,” *APL Phot.* **5**, 016107 (2020).
- [54] Mark Kremer, Ioannis Petrides, Eric Meyer, Matthias Heinrich, Oded Zilberberg, and Alexander Szameit, “A square-root topological insulator with non-quantized indices realized with photonic Aharonov-Bohm cages,” *Nat. Comm.* **11**, 907 (2020).
- [55] We point out that unlike 1D, the presence of several spatial directions may impose a constraint on the number of bands required to achieve MBFBL. For instance, the assumption of hopping between nearest neighbor unit cells in \mathcal{H}_{sp} implies that 2D MBFBL networks have to have three of more bands.
- [56] M. Röntgen, C. V. Morfonios, I. Brouzos, F. K. Diakonov, and P. Schmelcher, “Quantum network transfer and storage with compact localized states induced by local symmetries,” *Phys. Rev. Lett.* **123**, 080504 (2019).
- [57] Yoshihito Kuno, Takahiro Orito, and Ikuo Ichinose, “Flat-band many-body localization and ergodicity breaking in the Creutz ladder,” *New J. Phys.* **22**, 013032 (2020).
- [58] J. Jünemann, A. Piga, S.-J. Ran, M. Lewenstein, M. Rizzi, and A. Bermudez, “Exploring interacting topological insulators with ultracold atoms: The synthetic creutz-hubbard model,” *Phys. Rev. X* **7**, 031057 (2017).
- [59] Rubem Mondaini, G. G. Batrouni, and B. Grémaud, “Pairing and superconductivity in the flat band: Creutz lattice,” *Phys. Rev. B* **98**, 155142 (2018).
- [60] Murad Tovmasyan, Sebastiano Peotta, Long Liang, Päivi Törmä, and Sebastian D. Huber, “Prefomed pairs in flat bloch bands,” *Phys. Rev. B* **98**, 134513 (2018).
- [61] S Barbarino, D Rossini, M Rizzi, R Fazio, G E Santoro, and M Dalmonte, “Topological Devil’s staircase in atomic two-leg ladders,” *New J Phys.* **21**, 043048 (2019).
- [62] Nilanjan Roy, Ajith Ramachandran, and Auditya

- Sharma, “Compact, flat-band based, anderson and many-body localization in a diamond chain,” (2019), [arXiv:1912.09951 \[cond-mat.dis-nn\]](https://arxiv.org/abs/1912.09951).
- [63] Orito Takahiro, Kuno Yoshihito, and Ichinose Ikuo, “Exact projector hamiltonian, local integrals of motion, and many-body localization with topological order,” (2020), [arXiv:2004.07634 \[cond-mat.stat-mech\]](https://arxiv.org/abs/2004.07634).